

1 **Abilities of circumpapillary retinal nerve fiber layer thickness and vascular**  
2 **density to discriminate stages in primary open-angle glaucoma**

3

4 **Katsuya Yamaguchi<sup>1</sup>, Ryo Tomita<sup>1\*</sup>, Yoshito Koyanagi<sup>1</sup>, Kazuhide Kawase<sup>1</sup>, Ryo**  
5 **Asaoka<sup>2</sup>, Hiroko Terasaki<sup>1</sup>, Takeshi Iwase<sup>1,3</sup>, Koji M. Nishiguchi<sup>1</sup>**

6

7 1, Department of Ophthalmology, Nagoya University Graduate School of Medicine, 65  
8 Tsurumai-cho, Showa-ku, Nagoya, Aichi, 466-8560, Japan

9 2, Department of Ophthalmology, Seirei Hamamatsu General Hospital, 2-12-12  
10 Sumiyoshi, Naka-ku, Hamamatsu, Shizuoka, 430-8558, Japan

11 3, Department of Ophthalmology, Akita University Graduate School of Medicine, 1-1-1  
12 Hondou, Akita, 010-8543, Japan

13

14 \*Correspondence:

15 Ryo Tomita, Department of Ophthalmology, Nagoya University Graduate School of  
16 Medicine, 65 Tsurumai-cho, Showa-ku, Nagoya, Aichi, 466-8560, Japan

17 Tel: 81-52-744-2275; Fax: 81-52-744-2278

18 Email: [tomitaryo@med.nagoya-u.ac.jp](mailto:tomitaryo@med.nagoya-u.ac.jp)

19 Number of figures and tables: 4 figures and 3 tables.

20

21 **Key messages**

22 ***What is known:***

- 23 ● Circumpapillary retinal nerve fiber layer thickness (cpRNFLT) determined by  
24 optical coherence tomography (OCT) reaches a floor where further thinning cannot  
25 be detected if glaucoma is moderate to severe, whereas circumpapillary vessel  
26 density (cpVD) determined by OCT-angiography is less affected by the floor effect,  
27 even in severe cases. The differences in the ability of cpRNFLT and cpVD to  
28 discriminate glaucoma severities and to estimate visual field are unknown.

29 ***What is new:***

- 30 ● The ability to distinguish between moderate and severe glaucoma was higher for  
31 cpVD. cpVD is better for follow-ups after moderate stage.
- 32 ● The mean absolute error in estimating the visual field from both cpRNFLT and  
33 cpVD was significantly less than the error from cpRNFLT alone. The combination  
34 of cpRNFLT and cpVD may improve visual field estimation.

35

36 **Abstract**

37 **Purpose:** To clarify the abilities of circumpapillary retinal nerve fiber layer thickness  
38 (cpRNFLT) obtained by optical coherence tomography (OCT) and circumpapillary  
39 vessel density (cpVD) measured by OCT-angiography to distinguish different stages in  
40 primary open-angle glaucoma determined by 24-2 or 30-2 static visual field (VF)  
41 testing.

42 **Methods:** This retrospective study includes 25 healthy normal eyes of 25 subjects and  
43 87 primary open-angle glaucoma eyes of 87 patients. Areas under the receiver  
44 operating characteristic curves (AUROC) were evaluated for determining glaucoma  
45 stages using cpRNFLT and cpVD. The absolute errors of the estimated mean total  
46 deviation (mTD) using optimal models with cpRNFLT and cpVD were also compared.

47 **Results:** The AUROCs for discriminating glaucomatous eyes from normal eyes was  
48 significantly higher for cpRNFLT than the respective AUROCs for cpVD (0.969 [95% CI  
49 0.939 to 0.998] vs. 0.872 [95% CI 0.806 to 0.938],  $p = 0.006$ ), whereas cpVD had  
50 significantly higher AUROC for discriminating severe glaucoma eyes from moderate  
51 glaucoma eyes than cpRNFLT (0.771 [95% CI 0.655 to 0.886] vs. 0.578 [95% CI 0.420  
52 to 0.736],  $p = 0.022$ ). The mean absolute error in estimating mTD using both cpRNFLT  
53 and cpVD was significantly less than the error using cpRNFLT alone ( $4.56 \pm 3.76$  dB

54 vs.  $5.39 \pm 4.00$  dB,  $p = 0.027$ ).

55 **Conclusion:** Our results suggest that cpVD is better for follow-ups after moderate  
56 stage. The combination of cpRNFLT and cpVD may improve VF estimation compared  
57 to cpRNFLT alone.

58

59 **Keywords**

60 Glaucoma; OCT; OCT angiography; cpVD; cpRNFLT

61

62

## 63 **Introduction**

64 Glaucoma causes progressive visual field (VF) damage, which can significantly impact  
65 patient quality of life [1]. Because VF testing is subjective, fluctuations in results or  
66 difficulties in conducting the test often arise [2]. Therefore, objective measurements,  
67 which can accurately estimate glaucomatous VF defects, are essential. Circumpapillary  
68 retinal nerve fiber layer thickness (cpRNFLT) measured using optical coherence  
69 tomography (OCT) is a valuable glaucoma diagnostic tool [3, 4]. Reductions in  
70 cpRNFLT correlate well with the degree of glaucomatous VF damage, especially in the  
71 early stages of glaucoma [5]. However, the use of cpRNFLT in the clinic is problematic.  
72 Progression of severe glaucoma is difficult to detect due to the “floor effect” [6-8], which  
73 is observed in measurements with limited dynamic ranges. For instance, in the severe  
74 stages of glaucoma, the actual progression of glaucoma may be misinterpreted as  
75 stability because cpRNFLT has reached the measurement range floor. Thus,  
76 measurement of cpRNFLT by OCT may be valuable in the early stages of glaucoma  
77 but not in the severe stages.

78       Circumpapillary vessel density (cpVD) measured by OCT angiography (OCTA)  
79 may be useful[9] for monitoring severe glaucoma because cpVD is less likely to suffer  
80 from a floor effect than cpRNFLT [10, 11]. Conversely, the diagnostic performance of

81 cpVD in early glaucoma is controversial; some reports demonstrate that cpVD is  
82 equivalent to cpRNFLT, while others report that cpVD is inferior to cpRNFLT [12-14].

83 Thus, the diagnostic ability and characteristics of cpRNFLT and cpVD at  
84 different glaucoma stages are controversial. Additionally, few comparative studies have  
85 examined the ability of cpRNFLT and cpVD to estimate VF defects [15, 16]. The  
86 purpose of this study was to compare the discriminating performance of cpRNFLT and  
87 cpVD at each stage in eyes with primary open-angle glaucoma (POAG) and normal  
88 eyes and evaluate the ability of cpRNFLT and cpVD to estimate VF damage.

89

## 90 **Methods**

91 This retrospective, observational comparative, single-center study was conducted in  
92 adherence to the tenets of the Declaration of Helsinki. The procedures were approved  
93 by the Institutional Review Board and the Ethics Committee of the Nagoya University  
94 Graduate School of Medicine. The institutional review board exempted this study from  
95 informed consent due to the retrospective study design. We published the study  
96 protocol on the website and offered participants the opportunity to opt out. The medical  
97 records of all patients who were diagnosed solely with POAG and consecutive patients  
98 with normal eyes who underwent routine eye examinations and had no ocular disease  
99 except for cataract or a history of vitreous disease such as epiretinal membrane or

100 retinal break in the opposite eye were evaluated. Patients who were examined within  
101 six months for OCT, OCTA, and VF at the Nagoya University Hospital from February  
102 2017 to November 2021 were included in the study as a convenience sample. The  
103 Standards for Reporting of Diagnostic Accuracy Studies (STARD) checklist for this  
104 study is shown as a supplementary information.[17]

105           Glaucoma specialists (KY and RT) classified normal eyes and POAG eyes  
106 while being blinded to the clinical information of the eyes, except for the parameters  
107 used in the following criteria. The criteria for normal eyes were: (1) normal findings in  
108 slit-lamp and ophthalmoscopic examinations; (2) best-corrected visual acuity (BCVA)  
109 better than 20/25; (3) intraocular pressure (IOP)  $\leq$  21 mmHg; and (4) normal VF of the  
110 Anderson–Patella classification; (5) age  $>20$  years. The criteria for eyes with POAG  
111 included: (1) the presence of glaucomatous optic disc changes determined by  
112 biomicroscopy, VF defects, and abnormal cpRNFL thinning determined by Cirrus OCT  
113 with embedded software, (2) open-angle determined by gonioscopy, and (3) age  $>20$   
114 years. Eyes in the POAG group were classified into three groups according to the  
115 degree of VF impairment: early, mean deviation (MD)  $> -6$  dB; moderate,  $-12$  dB  $<$  MD  
116  $< -6$  dB; and severe, MD  $< -12$  dB. The VFs were determined using a Humphrey Field  
117 Analyzer II (HFA; Carl Zeiss Meditec AG, Jena, Germany) and the Swedish interactive



118 threshold algorithm standard central 24-2 and 30-2 program. The mean total deviation  
119 of common 58 points of both 24-2 and 30-2 VF tests was recorded as an objective  
120 measure of the VF and expressed as mean total deviation (mTD). Only reliable VF  
121 tests were used; examinations with 20% fixation errors and > 33% false-positives or  
122 false-negatives were excluded.

### 123 **Exclusion criteria**

124 Patients with a history of systemic or ocular disease affecting the blood flow or  
125 structure of the retina were excluded from the study. In addition, eyes with severe  
126 cataracts or high myopia (axial length longer than 27 mm) were excluded. Eyes with  
127 IOP > 21 mm Hg on the test day were also excluded because high IOP may affect the  
128 measurement of cpVD[18, 19].

### 129 **Measurements of clinical parameters**

130 All subjects underwent ophthalmologic and general examinations that included the  
131 following: slit-lamp and ophthalmoscopic examinations, gonioscopy, IOP  
132 measurements, perimetry, spectral domain-OCT (SD-OCT) examinations, and swept  
133 source-OCTA (SS-OCTA) examination within six months. The decimal BCVA was  
134 converted to the logarithm of the minimum angle of resolution (logMAR) units for  
135 statistical analyses. The axial lengths were measured using partial optical coherence  
136 interferometry (IOL Master; Carl Zeiss Meditec, La Jolla, CA). The IOP was measured

137 with a handheld tonometer (Icare; Tiolat Oy, Helsinki, Finland).

### 138 **Measuring circumpapillary retinal nerve fiber layer thickness**

139 The global cpRNFLT was measured using the manufacturer's software with a SD-OCT  
140 system (CIRRUS HD-OCT 5000, Carl Zeiss AG, German). Poor quality images caused  
141 by artifacts, poor centration, and signal strength < 7 were excluded from the analyses.

### 142 **Measurement of circumpapillary vessel density**

143 Microcirculation images were obtained by the SS-OCTA system (Plex Elite 9000, Carl  
144 Zeiss AG, German). The global cpVD in the peripapillary nerve fiber layer within a 6-  
145 mm diameter circle centered on the optic papilla was calculated by the instrument  
146 software and prototype analysis vessel density quantification software (Peripapillary  
147 Nerve Fiber Layer Microvasculature Density v0.10, ARI Network Hub, Carl Zeiss  
148 Meditec Inc., Dublin, CA, USA) supplied by the manufacturer. The central region within  
149 a 6mm diameter circle, specifically a 2mm diameter area at the center, was excluded  
150 from the measurement, and major vessels were also excluded. Low-quality images,  
151 images with the center of the image misaligned with the optic disc, and images with  
152 signal strength < 7 were excluded.

### 153 **Statistical Analysis**

154 All data are reported as means  $\pm$  standard deviation (SD) unless otherwise specified.

155 One eye was randomly selected if data existed for both of the patient's eyes. Baseline

156 characteristics were compared using the one-way ANOVA. Scatterplots for cpRNFLT  
157 and cpVD were compared with scatterplots for mTD. The linear splines were expressed  
158 with locally weighted scatterplot smoothing (LOWESS) curves. Receiver operating  
159 characteristic (ROC) curves were drawn based on a logistic regression analysis of the  
160 ability of cpRNFLT and cpVD to differentiate between normal eyes and the different  
161 stages of glaucoma. The area under the receiver operating characteristic curves  
162 (AUROC) were compared between cpRNFL and cpVD using the Delong test. Single or  
163 multiple regression analyses with leave-one-out cross-validation were conducted to  
164 estimate mTD based on cpRNFLT and/or cpVD. Each model was trained on all eyes  
165 except one eye as test data. When the model was adapted to the test data, the  
166 estimated value was determined and repeated to obtain the estimated value for all  
167 patients included in the study. The absolute error was defined as the absolute  
168 difference between the actual mTD and estimated mTD calculated using the regression  
169 model obtained with leave-one-out cross-validation. The absolute errors in cpRNFL  
170 and/or cpVD were compared using the one-way ANOVA and the Tukey test for multiple  
171 comparisons. The statistical programming language R (V.4.1.2, The R Foundation for  
172 Statistical Computing, Vienna, Austria) was used for all statistical analyses. A p-value <  
173 0.05 was considered statistically significant.

174

175 **Results**

176 Data were obtained from 43 eyes of 34 healthy subjects and 223 eyes of 133  
177 glaucoma patients. After excluding eyes that did not meet the criterion and randomly  
178 selecting one eye if two eyes were included per patient, a total of 112 eyes from 112  
179 subjects were analyzed (Figure 1), including 25 eyes from 25 healthy subjects, 24 eyes  
180 with early glaucoma from 24 patients, 22 eyes with moderate glaucoma from 22  
181 patients, and 41 eyes with severe glaucoma from 41 patients. Table 1 shows the  
182 baseline clinical characteristics of the study subjects. There were significant differences  
183 in visual acuity, IOP, MD, and mTD values among severity levels. The cpRNFLT  
184 obtained by SD-OCT were  $93.7 \pm 9.5 \mu\text{m}$  for normal eyes,  $74.4 \pm 9.5 \mu\text{m}$  for eyes with  
185 early glaucoma,  $67.5 \pm 11.4 \mu\text{m}$  for eyes with moderate glaucoma, and  $63.5 \pm 7.7 \mu\text{m}$   
186 for eyes with severe glaucoma (Table 2). The cpRNFLT of any glaucoma severity were  
187 significantly less than the cpRNFLT of normal eyes (all,  $p < 0.001$ ). The cpRNFLT of  
188 eyes with severe glaucoma was significantly less than the cpRNFLT of eyes with early  
189 glaucoma ( $p < 0.001$ ). The cpVDs obtained by SS-OCTA were  $54.7 \pm 1.4\%$  in normal  
190 eyes and  $52.4 \pm 2.6\%$ ,  $52.0 \pm 2.4\%$ , and  $49.0 \pm 3.4\%$  in eyes with early, moderate, and  
191 severe glaucoma, respectively, and these cpVDs were significantly lower than that of

192 normal eyes (all,  $p < 0.001$ ). The cpVD of eyes with severe glaucoma was significantly  
193 lower than the cpVDs of eyes with early and moderate glaucoma (all,  $p < 0.001$ ).

194 The AUROC based on logistic regression analysis discriminating all eyes with  
195 glaucoma from normal eyes by cpRNFLT (0.969, 95% CI: 0.939–0.998) was  
196 significantly higher than the AUROC for the cpVD (0.872, 95% CI: 0.806–0.938,  $p =$   
197 0.006; Figure 2A, Table 3). The AUROC discriminating eyes with early glaucoma from  
198 normal eyes by cpRNFLT (0.929, 95% CI: 0.844–1.000) was higher than the AUROC  
199 for cpVD (0.783, 95% CI: 0.654–0.913), but not significantly ( $p = 0.073$ ; Figure 2B).  
200 AUROCs discriminating eyes with moderate glaucoma from eyes with early glaucoma  
201 using cpRNFLT (0.710, 95% CI: 0.552–0.869) and cpVD (0.576, 95% CI: 0.405–0.747)  
202 were not significantly different (Figure 2C). The AUROC discriminating eyes with  
203 severe glaucoma from eyes with moderate glaucoma using cpVD (0.771, 95% CI:  
204 0.655–0.886) was significantly higher than the AUROC using cpRNFLT (0.578, 95% CI:  
205 0.420–0.736,  $p = 0.022$ ; Figure 2D).

206 Figure 3 shows the relationship between mTD and cpRNFLT and cpVD in all  
207 eyes. It was found that cpRNFLT and cpVD were significantly correlated with mTD ( $r =$   
208 0.635;  $p < 0.001$  and  $r = 0.657$ ;  $p < 0.001$ , respectively) in all eyes. In normal eyes and  
209 eyes with early and moderate glaucoma, cpRNFLT significantly correlated with mTD ( $r$

210 = 0.598,  $p < 0.001$ ). However, no significant correlation was observed between  
211 cpRNFLT and mTD for eyes with severe glaucoma ( $r = 0.203$ ,  $p = 0.204$ ). On the other  
212 hand, a significant correlation was detected between cpVD and mTD in normal eyes  
213 and eyes with early and moderate glaucoma ( $r = 0.377$ ,  $p = 0.001$ ) and also in eyes  
214 with severe glaucoma ( $r = 0.417$ ,  $p = 0.007$ ).

215           The mean absolute error calculated using the regression model with both  
216 cpRNFLT and cpVD ( $4.56 \pm 3.76$  dB) was significantly less than the absolute error  
217 calculated with cpRNFLT only ( $5.39 \pm 4.00$  dB,  $p = 0.027$ ; Figure 4), but not significantly  
218 less than the absolute error calculated with cpVD only ( $5.17 \pm 4.08$  dB,  $p = 0.142$ ). The  
219 model for estimating mTD from all cases with both cpRNFLT and cpVD is as follows:  
220  $mTD = -84.4 + 1.12 \times cpVD$  (Standard Error [SE] = 0.188,  $p < 0.001$ ) +  $0.233 \times$   
221 cpRNFLT (SE = 0.0435,  $p < 0.001$ ). The model for estimating mTD from all cases with  
222 cpRNFLT alone is:  $mTD = -36.4 + 0.367 \times cpRNFLT$  (SE = 0.0426,  $p < 0.001$ ). The  
223 model for estimating mTD from all cases with cpVD alone is:  $mTD = -94.3 + 1.65 \times$   
224 cpVD (SE = 0.180,  $p < 0.001$ ).

225

## 226 **Discussion**

227 In this study, we examined the ability of cpRNFLT and cpVD to distinguish stages of  
228 glaucoma. The AUROCs using cpVD were significantly better at discriminating between

229 moderate and severe glaucoma. In eyes with severe glaucoma, cpVD significantly  
230 correlated with mTD, whereas cpRNFLT did not correlate with mTD. The mean  
231 absolute error in estimating mTD using both cpRNFLT and cpVD was significantly less  
232 than the error using cpRNFLT alone.

233         The relationship between cpVD and VF damages has been described in  
234 previous reports [9, 20, 21]. Several reports indicate that the abilities of cpVD and  
235 cpRNFLT to diagnose early glaucoma are similar, while other reports indicate that  
236 cpRNFLT is better at diagnosing early glaucoma [12, 22, 23]. In this study, the AUROC  
237 for differentiating eyes with early glaucoma from normal eyes using cpVD (0.872) was  
238 not significantly but lower than the AUROC for cpRNFL (0.969). The AUROC values for  
239 cpVD in previous reports vary but were roughly consistent with the values in the  
240 present study [12, 13, 22]. Lee et al. suggested that the primary change in early  
241 glaucoma is a decrease in cpRNFLT, and the decrease in cpVD may be a secondary  
242 change, which may explain the superiority of cpRNFL in diagnosing early glaucoma  
243 [24]. However, whether nerve dropout or reduced blood flow comes first in glaucoma is  
244 still controversial. In contrast, the discriminating performance of cpRNFLT is inferior in  
245 severe glaucoma relative to early glaucoma due to the floor effect [25]. In this study,  
246 the AUROC differentiating eyes with severe glaucoma from eyes with moderate

247 glaucoma using cpRNFLT was significantly lower than the AUROC using cpVD. To our  
248 knowledge, no reports compare the ability of cpVD and cpRNFLT to discriminate  
249 between eyes with moderate and severe glaucoma. However, the lack of a floor effect  
250 in cpVD until the disease is more severe is reasonable. Phillips et al. reported that  
251 cpRNFLT obtained by OCT floored earlier (MD: -17.8dB) than the peripapillary vessel  
252 density obtained by OCTA (MD: -26.6dB) [11]. Moghimi et al. also indicated the  
253 superiority of OCTA with respect to the floor effect. In the study, cpRNFLT reached the  
254 floor at an MD value of -17.5 dB, while no floor was detected in cpVD [10]. Additionally,  
255 cpRNFLT did not significantly correlate with mTD in cases of severe glaucoma,  
256 whereas cpVD significantly correlated with mTD even in cases of severe glaucoma.  
257 The difference between these two correlations may be due to the floor effect [26]. The  
258 results of this study suggest that cpVD is better for follow-ups after the moderate stage.  
259 Therefore, the difference in efficacy between cpRNFLT and cpVD depending on the  
260 severity of glaucoma is useful for understanding the function versus structure  
261 relationship in glaucoma.

262           The absolute error between the actual mTD and the estimated mTD from the  
263 regression model using both cpRNFLT and cpVD was significantly less than the error  
264 using cpRNFLT values alone. This result suggests that the combination of cpRNFLT



265 and cpVD may be more effective in estimating glaucomatous VF defects than cpRNFLT  
266 only. Several studies have attempted to predict glaucomatous VF damage from  
267 structure using cpRNFLT [27-30]. But only a few studies have used OCTA [16, 31].  
268 Wong et al. reported that combining OCT and OCTA improves the modeling of local VF  
269 defects in early glaucoma [31]. To the best of our knowledge, this is the first study to  
270 predict VF from OCT and OCTA parameters, including many severe cases. However,  
271 the mean absolute error between the predicted mTD and actual mTD values was  
272 relatively large in this study. The large errors may be because of using the image of the  
273 whole area around the optic disc for estimating VF and including many eyes with  
274 severe glaucoma and a small number of cases relative to previous studies. Further  
275 research should be conducted to find a more appropriate estimation model using the  
276 combination of cpRNFLT and cpVD.

277           There are several limitations to this study. First, this study excluded highly  
278 myopic eyes. Shin et al. reported that the cpVD correlates better with VF than  
279 cpRNFLT in patients with glaucoma and high myopia [32]. Further studies of  
280 diagnostic performance in high myopia are needed. Second, only one VF and  
281 imaging test was performed. In addition to the variability in the VF test results,  
282 cpRNFLT and cpVD may also vary due to changes in image quality and

283 physiological blood flow. Especially, the variability of the results of them in  
284 moderate to severe glaucoma may be significant. Thus, we defined exclusion  
285 criteria for VF testing and images to avoid this effect as much as possible. Third,  
286 this study is based on the image of the whole area around the optic disc and the  
287 global VF. The cpRNFL and cpVD of the nasal retina, which are less affected by  
288 VF measurement points, are also measured in the same way as the more critical  
289 temporal retina. A more detailed sectoral study corresponding to the VF may be  
290 needed. Fourth, the OCT, OCTA, and VF measurements in this study were  
291 performed within 6 months. Therefore, if visual field or structural disorders  
292 progress during this time, there may be a discrepancy in the results. Fifth, thinning  
293 of the cpRNFL by OCT was used as a selection criterion for eyes with glaucoma.  
294 This may lead to incorporation bias in tests such as diagnostic ability. This bias  
295 may overestimate the sensitivity, specificity, and AUC of cpRNFLT in tests where  
296 cpRNFLT distinguishes between severities, especially in distinguishing between  
297 normal eyes and all eyes with glaucoma, and between normal eyes and eyes with  
298 early glaucoma. The superiority of cpRNFLT over cpVD in distinguishing between  
299 normal eyes and all eyes with glaucoma and between normal eyes and eyes with  
300 early glaucoma may be also overestimated.

301            In conclusion, cpVD was superior in distinguishing between moderate and  
302 severe glaucoma. The mean absolute error of the estimated mTD based on the  
303 combination of cpRNFLT and cpVD was significantly less than the absolute error using  
304 cpRNFLT alone, suggesting that the complementary use of the two measurements may  
305 be useful in estimating the severity of glaucoma.

306

307 **Compliance with Ethical Standards**

308 **Funding:** This work was supported by a Grant-in-Aid for Young Scientists (R.T.,  
309 number 21K16870) from JSPS KAKENHI (<http://www.jsps.go.jp/>).

310 **Competing interests:** KY, None; RT, None; YK, None; KK received honoraria for  
311 lectures from Senju; RA, None; HT received non-financial research support from Carl  
312 Zeiss related to swept source optical coherence tomography and grants and honoraria  
313 for lectures from Otsuka, Kowa, Santen, Senju, Sanofi, Alcon, Novartis, ROHTO, and  
314 Wakamoto. She received grants and consulting fees from Bayer and honoraria for  
315 lectures from HOYA and Johnson & Johnson; TI, None; KN received grants from  
316 Takara bio, Takeda pharmaceutical, JCR Pharma, Alcon, and Bayer, and honoraria for  
317 lectures from Novartis, Santen, Chugai Pharma, Kowa, Senju, Otsuka, and Wakamoto.  
318 He has a patent related to a single AAV vector.

319 **Acknowledgments:** The swept source optical coherence tomography device used in  
320 this study was on loan from Carl Zeiss Meditec.

321 **Standards of reporting:** The Standards for Reporting of Diagnostic Accuracy Studies  
322 (STARD) checklist for this study is shown as a supplementary information.[17]

323 **Ethical approval:** This study was conducted in adherence to the tenets of the  
324 Declaration of Helsinki. The procedures were approved by the Institutional Review  
325 Board and the Ethics Committee of the Nagoya University Graduate School of

326 Medicine.

327 **Informed consent:** The institutional review board exempted this study from informed  
328 consent due to the retrospective study design. We published the study protocol on the  
329 website and offered participants the opportunity to opt out.

330 **Author Contributions:** KY, RT, TI and KN were involved in the design and conduct of  
331 the study; KY, RT, and TI were involved in the collection, management, analysis, and  
332 interpretation of data; and KY, RT, KK, RA, HT, TI, and KN were involved in the  
333 preparation, review, and approval of the manuscript.

334

335

336 **References**

- 337 1. Altangerel U, Spaeth GL, Rhee DJ (2003) Visual function, disability, and  
338 psychological impact of glaucoma. *Current opinion in ophthalmology* 14:100-  
339 105 doi: 10.1097/00055735-200304000-00009
- 340 2. Flammer J, Drance SM, Zulauf M (1984) Differential light threshold: short-and  
341 long-term fluctuation in patients with glaucoma, normal controls, and  
342 patients with suspected glaucoma. *Archives of ophthalmology* 102:704-706
- 343 3. Fujino Y, Murata H, Matsuura M et al (2018) Mapping the Central 10° Visual  
344 Field to the Optic Nerve Head Using the Structure-Function Relationship.  
345 *Investigative Ophthalmology & Visual Science* 59:2801-2807 doi:  
346 10.1167/iovs.17-23485
- 347 4. Garway-Heath DF, Poinosawmy D, Fitzke FW, Hitchings RA (2000) Mapping  
348 the visual field to the optic disc in normal tension glaucoma eyes.  
349 *Ophthalmology* 107:1809-1815 doi: 10.1016/s0161-6420(00)00284-0
- 350 5. Malik R, Swanson WH, Garway-Heath DF (2012) 'Structure-function  
351 relationship' in glaucoma: past thinking and current concepts. *Clinical &*  
352 *Experimental Ophthalmology* 40:369-380 doi: [https://doi.org/10.1111/j.1442-  
353 9071.2012.02770.x](https://doi.org/10.1111/j.1442-9071.2012.02770.x)
- 354 6. Mwanza J-C, Budenz DL, Warren JL, Webel AD, Reynolds CE, Barbosa DT, Lin S  
355 (2015) Retinal nerve fibre layer thickness floor and corresponding functional  
356 loss in glaucoma. *British Journal of Ophthalmology* 99:732-737 doi:  
357 10.1136/bjophthalmol-2014-305745
- 358 7. Blumenthal EZ, Horani A, Sasikumar R, Garudadri C, Udaykumar A, Thomas R  
359 (2006) Correlating structure with function in end-stage glaucoma.  
360 *Ophthalmic Surg Lasers Imaging* 37:218-223 doi: 10.3928/15428877-  
361 20060501-06
- 362 8. Hood DC, Kardon RH (2007) A framework for comparing structural and  
363 functional measures of glaucomatous damage. *Progress in Retinal and Eye*  
364 *Research* 26:688-710 doi: <https://doi.org/10.1016/j.preteyeres.2007.08.001>
- 365 9. Yarmohammadi A, Zangwill LM, Diniz-Filho A et al (2016) Relationship  
366 between Optical Coherence Tomography Angiography Vessel Density and  
367 Severity of Visual Field Loss in Glaucoma. *Ophthalmology* 123:2498-2508  
368 doi: <https://doi.org/10.1016/j.ophtha.2016.08.041>
- 369 10. Moghimi S, Bowd C, Zangwill LM et al (2019) Measurement Floors and  
370 Dynamic Ranges of OCT and OCT Angiography in Glaucoma. *Ophthalmology*

- 371 126:980-988 doi: 10.1016/j.opthta.2019.03.003
- 372 11. Phillips MJ, Dinh-Dang D, Bolo K et al (2021) Steps to Measurement Floor of  
373 an Optical Microangiography Device in Glaucoma. American Journal of  
374 Ophthalmology 231:58-69 doi: <https://doi.org/10.1016/j.ajo.2021.05.012>
- 375 12. Chung JK, Hwang YH, Wi JM, Kim M, Jung JJ (2017) Glaucoma Diagnostic  
376 Ability of the Optical Coherence Tomography Angiography Vessel Density  
377 Parameters. Current Eye Research 42:1458-1467 doi:  
378 10.1080/02713683.2017.1337157
- 379 13. Geyman LS, Garg RA, Suwan Y et al (2017) Peripapillary perfused capillary  
380 density in primary open<strong>-</strong>angle glaucoma across disease  
381 stage<strong>:</strong> an optical coherence tomography angiography  
382 study. British Journal of Ophthalmology 101:1261-1268 doi:  
383 10.1136/bjophthalmol-2016-309642
- 384 14. Akiyama K, Saito H, Shirato S et al (2022) Diagnostic ability and sectoral  
385 structure–function relationship of circumpapillary and macular superficial  
386 vessel density in early glaucomatous eyes. Scientific Reports 12:5991 doi:  
387 10.1038/s41598-022-10033-1
- 388 15. Yu HH, Maetschke SR, Antony BJ, Ishikawa H, Wollstein G, Schuman JS,  
389 Garnavi R (2021) Estimating Global Visual Field Indices in Glaucoma by  
390 Combining Macula and Optic Disc OCT Scans Using 3-Dimensional  
391 Convolutional Neural Networks. Ophthalmol Glaucoma 4:102-112 doi:  
392 10.1016/j.ogla.2020.07.002
- 393 16. Xu C, Saini C, Wang M et al (2023) Combined Model of OCT Angiography and  
394 Structural OCT Parameters to Predict Paracentral Visual Field Loss in Primary  
395 Open-Angle Glaucoma. Ophthalmology Glaucoma 6:255-265 doi:  
396 <https://doi.org/10.1016/j.ogla.2022.10.001>
- 397 17. Cohen JF, Korevaar DA, Altman DG et al (2016) STARD 2015 guidelines for  
398 reporting diagnostic accuracy studies: explanation and elaboration. BMJ  
399 Open 6:e012799 doi: 10.1136/bmjopen-2016-012799
- 400 18. Wang X, Chen J, Kong X, Sun X (2020) Immediate Changes in Peripapillary  
401 Retinal Vasculature after Intraocular Pressure Elevation -an Optical  
402 Coherence Tomography Angiography Study. Curr Eye Res 45:749-756 doi:  
403 10.1080/02713683.2019.1695843
- 404 19. Holló G (2017) Influence of Large Intraocular Pressure Reduction on  
405 Peripapillary OCT Vessel Density in Ocular Hypertensive and Glaucoma Eyes.  
406 Journal of Glaucoma 26:e7-e10 doi: 10.1097/ijg.0000000000000527

- 407 20. Hong KL, Burkemper B, Urrea AL et al (2021) Hemiretinal Asymmetry in  
408 Peripapillary Vessel Density in Healthy, Glaucoma Suspect, and Glaucoma  
409 Eyes. *Am J Ophthalmol* 230:156-165 doi: 10.1016/j.ajo.2021.05.019
- 410 21. WuDunn D, Takusagawa HL, Sit AJ et al (2021) OCT Angiography for the  
411 Diagnosis of Glaucoma: A Report by the American Academy of  
412 Ophthalmology. *Ophthalmology* 128:1222-1235 doi:  
413 10.1016/j.ophtha.2020.12.027
- 414 22. Yarmohammadi A, Zangwill LM, Diniz-Filho A et al (2016) Optical Coherence  
415 Tomography Angiography Vessel Density in Healthy, Glaucoma Suspect, and  
416 Glaucoma Eyes. *Invest Ophthalmol Vis Sci* 57:Oct451-459 doi:  
417 10.1167/iovs.15-18944
- 418 23. Rao HL, Pradhan ZS, Weinreb RN et al (2017) A comparison of the diagnostic  
419 ability of vessel density and structural measurements of optical coherence  
420 tomography in primary open angle glaucoma. *PLOS ONE* 12:e0173930 doi:  
421 10.1371/journal.pone.0173930
- 422 24. Lee EJ, Lee KM, Lee SH, Kim TW (2016) OCT Angiography of the Peripapillary  
423 Retina in Primary Open-Angle Glaucoma. *Invest Ophthalmol Vis Sci* 57:6265-  
424 6270 doi: 10.1167/iovs.16-20287
- 425 25. Sihota R, Sony P, Gupta V, Dada T, Singh R (2006) Diagnostic Capability of  
426 Optical Coherence Tomography in Evaluating the Degree of Glaucomatous  
427 Retinal Nerve Fiber Damage. *Investigative Ophthalmology & Visual Science*  
428 47:2006-2010 doi: 10.1167/iovs.05-1102
- 429 26. Kuroda F, Iwase T, Yamamoto K, Ra E, Terasaki H (2020) Correlation between  
430 blood flow on optic nerve head and structural and functional changes in eyes  
431 with glaucoma. *Sci Rep* 10:729 doi: 10.1038/s41598-020-57583-w
- 432 27. Zhu H, Crabb DP, Schlottmann PG et al (2010) Predicting visual function from  
433 the measurements of retinal nerve fiber layer structure. *Invest Ophthalmol*  
434 *Vis Sci* 51:5657-5666 doi: 10.1167/iovs.10-5239
- 435 28. Christopher M, Bowd C, Belghith A et al (2020) Deep Learning Approaches  
436 Predict Glaucomatous Visual Field Damage from OCT Optic Nerve Head En  
437 Face Images and Retinal Nerve Fiber Layer Thickness Maps. *Ophthalmology*  
438 127:346-356 doi: 10.1016/j.ophtha.2019.09.036
- 439 29. Bogunović H, Kwon YH, Rashid A et al (2015) Relationships of Retinal  
440 Structure and Humphrey 24-2 Visual Field Thresholds in Patients With  
441 Glaucoma. *Investigative Ophthalmology & Visual Science* 56:259-271 doi:  
442 10.1167/iovs.14-15885



- 443 30. Hashimoto Y, Asaoka R, Kiwaki T et al (2021) Deep learning model to predict  
444 visual field in central 10° from optical coherence tomography measurement  
445 in glaucoma. *British Journal of Ophthalmology* 105:507-513 doi:  
446 10.1136/bjophthalmol-2019-315600
- 447 31. Wong D, Chua J, Tan B et al (2021) Combining OCT and OCTA for Focal  
448 Structure-Function Modeling in Early Primary Open-Angle Glaucoma.  
449 *Investigative Ophthalmology & Visual Science* 62:8-8 doi:  
450 10.1167/iovs.62.15.8
- 451 32. Shin JW, Kwon J, Lee J, Kook MS (2019) Relationship between vessel density  
452 and visual field sensitivity in glaucomatous eyes with high myopia. *British*  
453 *Journal of Ophthalmology* 103:585-591 doi: 10.1136/bjophthalmol-2018-  
454 312085
- 455

**Table 1. Demographics of subjects.**

	Control	POAG			<i>p</i> -value
		early	moderate	severe	
Number of eyes	25	24	22	41	
Sex, m/f	14 / 11	14 / 12	13 / 9	30 / 11	
Age, year	68.8 ±	67.6 ±	69.2 ±	69.3 ±	0.95
	11.2	11.7	12.1	11.0	0
Axial length, mm	24.6 ±	24.9 ±	24.7 ±	24.9 ±	0.56
	0.9	1.1	1.2	1.5	1
Visual acuity,	0.034 ±	0.039 ±	0.133 ±	0.199 ±	0.00
logMAR	0.076	0.143	0.174	0.311	7
Intraocular	14.4 ±	12.1 ±	11.1 ±	12.3 ±	0.02
pressure, mmHg	2.9	3.5	4.1	4.1	3
					<
Mean deviation,	-0.12 ±	-2.87 ±	-9.32 ±	-19.6 ±	0.00
dB	1.23	1.77	1.84	5.5	1
Mean total	-0.20 ±	-2.88 ±	-9.16 ±	-19.0 ±	<
deviation, dB	1.34	1.88	1.73	5.2	0.00

MAR, minimum angle of resolution; POAG, primary open-angle

glaucoma

456

457

**Table 2. Values of cpRNFLT and cpVD in normal eyes and each stage of glaucoma.**

	Control	POAG			<i>p</i> -value
		early	moderate	advanced	
Number of eyes	25	24	22	41	
cpRNFLT, $\mu\text{m}$	$93.7 \pm 9.5$	$74.4 \pm 9.5$	$67.5 \pm 11.4$	$63.5 \pm 7.7$	< 0.001
cpVD, %	$54.7 \pm 1.4$	$52.4 \pm 2.6$	$52.0 \pm 2.4$	$49.0 \pm 3.4$	< 0.001

POAG, primary open-angle glaucoma; cpRNFLT, circumpapillary retinal nerve fiber layer thickness; cpVD, circumpapillary vessel density

458

459

**Table 3. The area under the receiver operating characteristic curve of discriminating each stage of glaucoma.**

	cpRNFL		cpVD		p-value
	T				
	AUROC	95% CI	AUROC	95% CI	
normal (25 eyes) vs. glaucoma (87 eyes)	0.969	0.939–0.998	0.872	0.806–0.938	0.006
normal (25 eyes) vs. early glaucoma (24eyes)	0.929	0.844–1.000	0.783	0.654–0.913	0.073
early (24 eyes) vs. moderate glaucoma (22 eyes)	0.710	0.552–0.869	0.576	0.405–0.747	0.206
moderate (22 eyes) vs. severe glaucoma (41 eyes)	0.578	0.420–0.736	0.771	0.655–0.886	0.022

cpRNFLT, circumpapillary retinal nerve fiber layer thickness; cpVD, circumpapillary

---

vessel density; AUROC, area under the receiver operating characteristic curve

460

461

462 **Figure Legends**

463 **Figure 1** Study subjects flow chart.

464

465 **Figure 2** Receiver operating characteristic (ROC) curves of cpRNFLT and cpVD for  
466 discriminating each stage of glaucoma. **(A)** ROC curves for discriminating all eyes with  
467 glaucoma from normal eyes. The areas under the ROCs (AUROCs) were 0.969 (95%  
468 confidence interval (CI) 0.939–0.998) for cpRNFLT and 0.872 (95% CI 0.806–0.938) for  
469 cpVD ( $p = 0.006$ ). **(B)** The ROC curves for discriminating eyes with early glaucoma  
470 from normal eyes. The AUROCs were 0.929 (95% CI 0.844–1.000) for cpRNFLT and  
471 0.783 (95% CI 0.654–0.913) for cpVD ( $p = 0.073$ ). **(C)** The ROC curves for  
472 discriminating eyes with moderate glaucoma from eyes with early glaucoma. The  
473 AUROCs were 0.710 (95% CI 0.552–0.869) for cpRNFLT and 0.576 (95% CI 0.405–  
474 0.747) for cpVD ( $p = 0.206$ ). **(D)** The ROC curves for discriminating severe glaucoma  
475 eyes from moderate eyes. The AUROCs were 0.578 (95% CI 0.420–0.736) for  
476 cpRNFLT and 0.771 (95% CI 0.655–0.886) for cpVD ( $p = 0.022$ ). cpRNFLT:

477 circumpapillary retinal nerve fiber layer thickness; cpVD: circumpapillary vessel density  
478

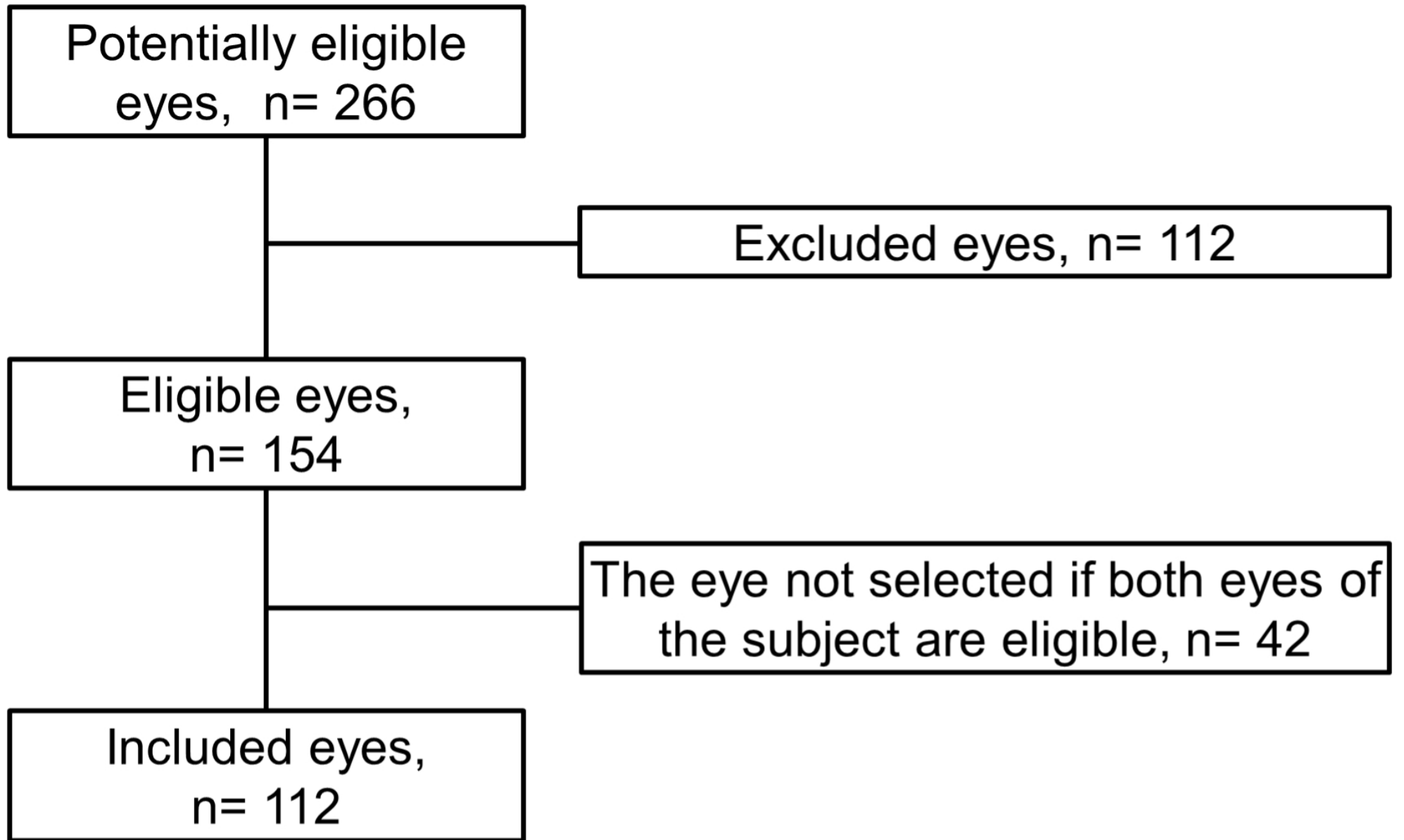
479 **Figure 3** Scatterplots with locally weighted scatterplot smoothing curves showing the  
480 relationship between mean total deviation (mTD) and cpRNFLT **(A)** and cpVD **(B)**. With  
481 more severe mTD, cpRNFLT showed little change with decreasing mTD, but cpVD did  
482 not show changes. Between cpRNFLT and mTD, a significant correlation was detected  
483 in normal eyes and eyes with early and moderate glaucoma ( $r = 0.598$ ,  $p < 0.001$ ), but  
484 no significant correlation was detected in eyes with severe glaucoma ( $r = 0.203$ ,  $p =$   
485 0.204). Between cpVD and mTD, a significant correlation was detected in normal eyes  
486 and eyes with early and moderate glaucoma ( $r = 0.377$ ,  $p = 0.001$ ) and in eyes with  
487 severe glaucoma ( $r = 0.417$ ,  $p = 0.007$ ).

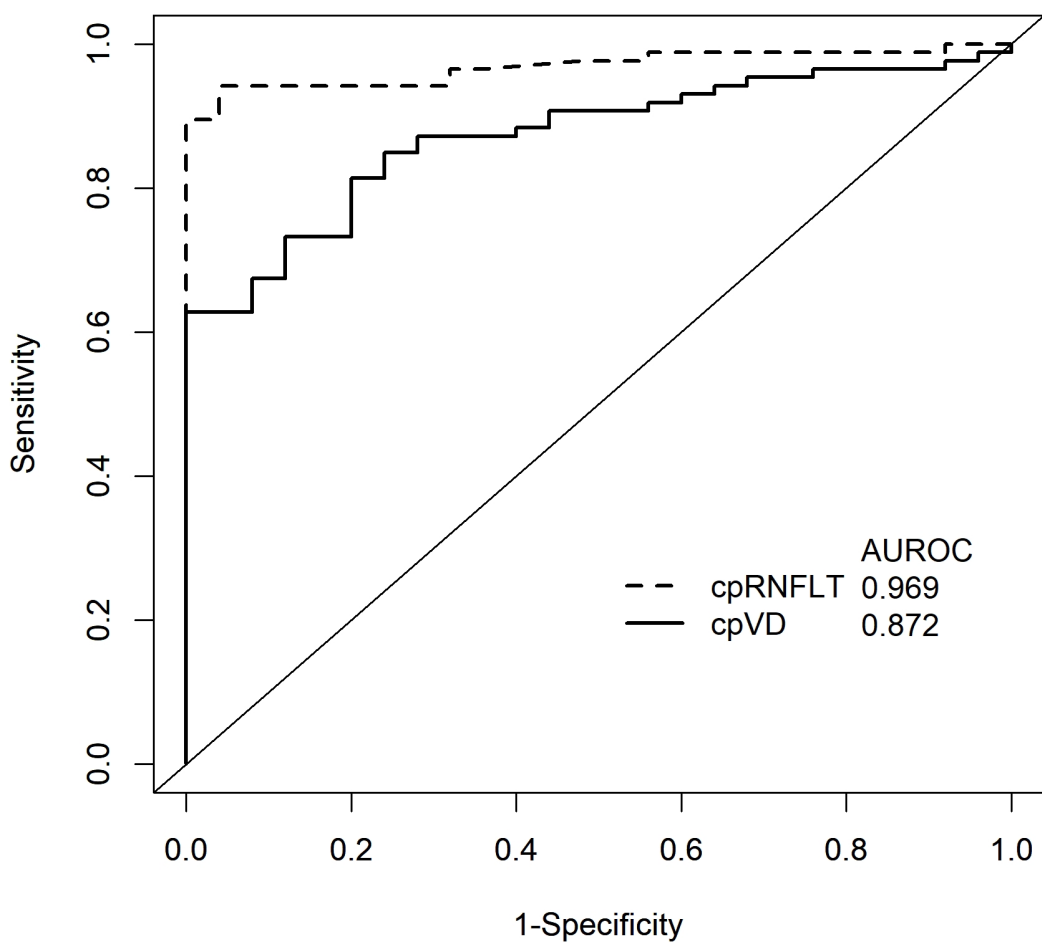
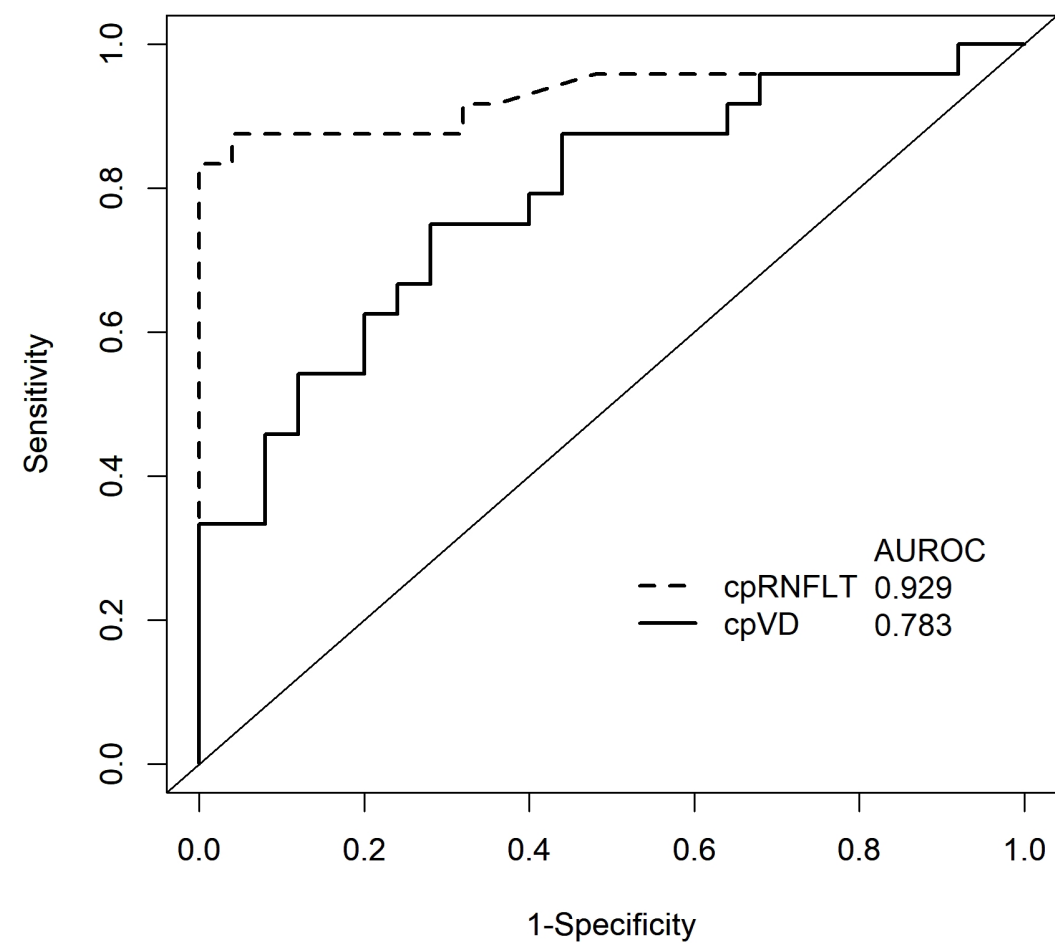
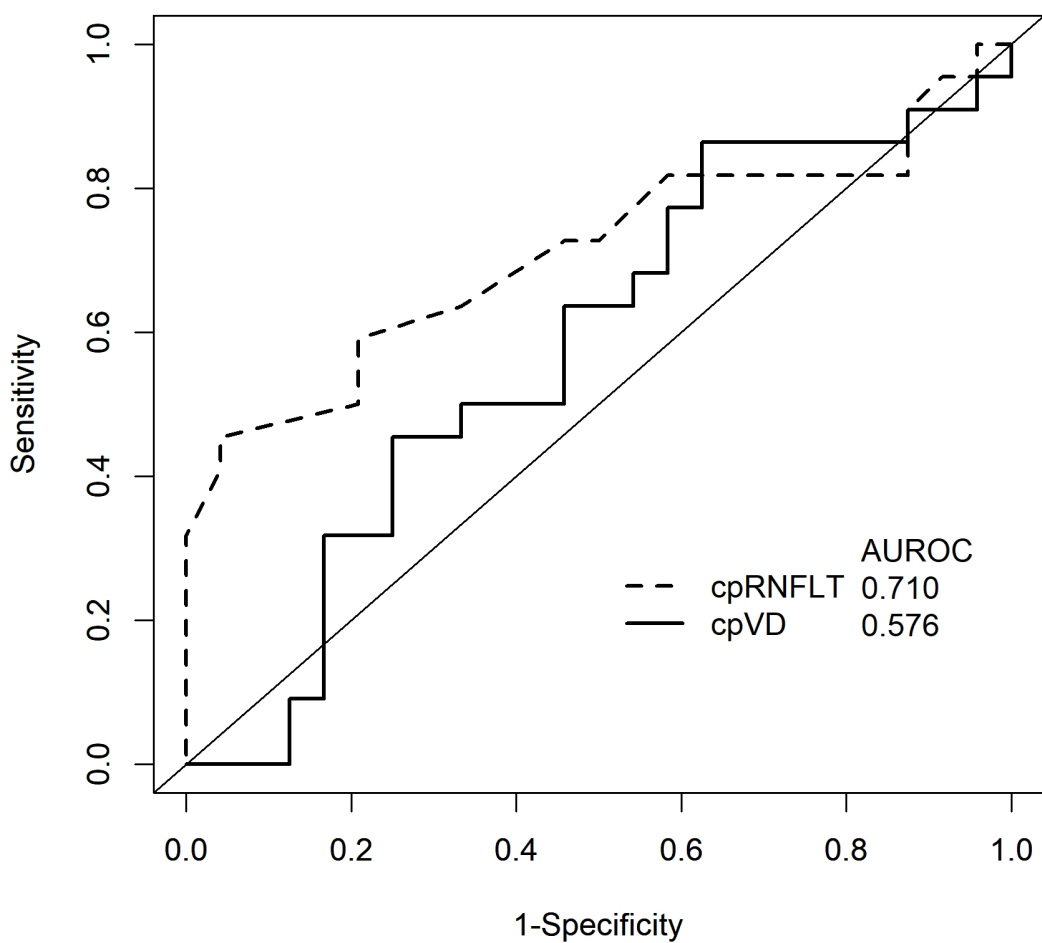
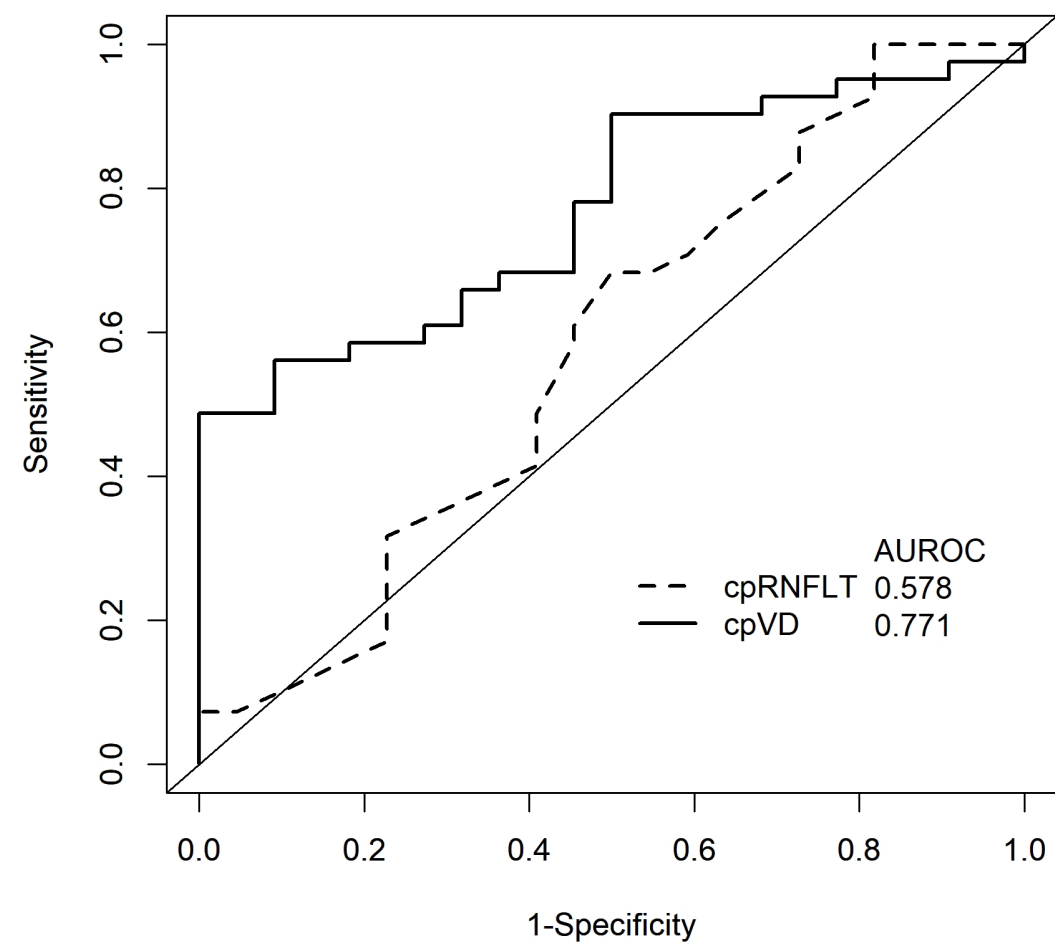
488 cpRNFLT: circumpapillary retinal nerve fiber layer thickness; cpVD: circumpapillary  
489 vessel density  
490

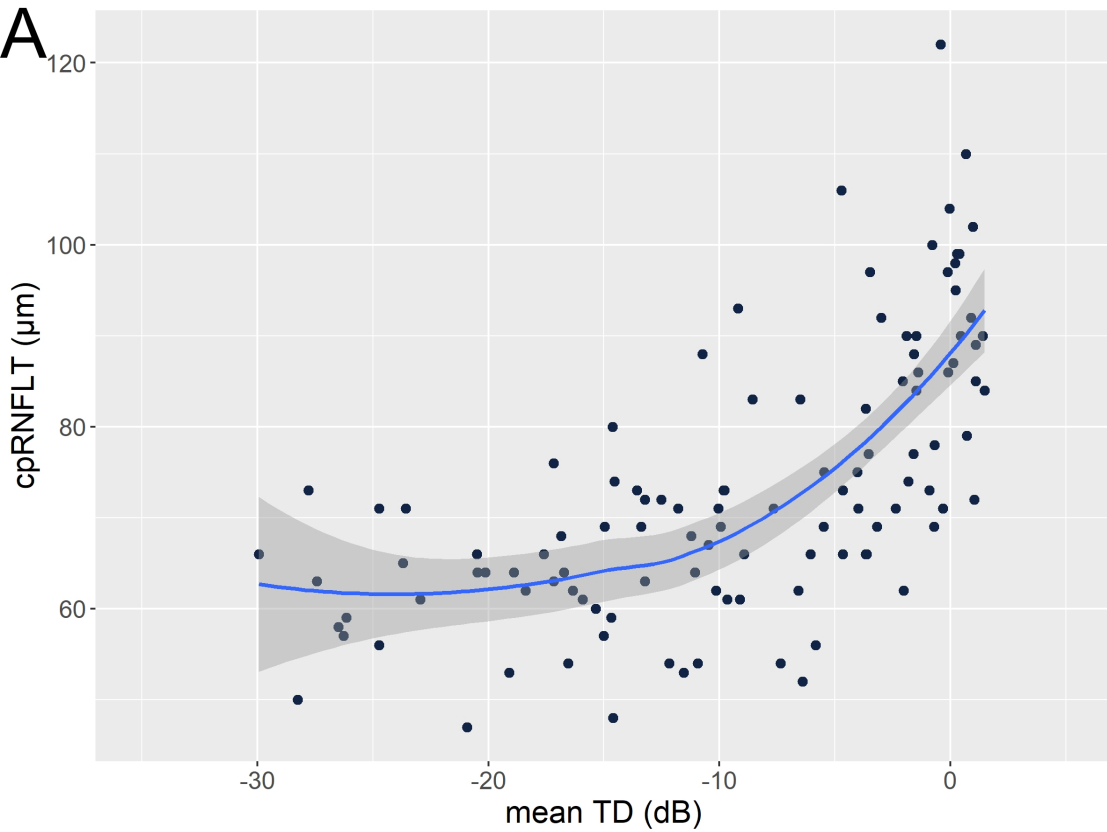
491 **Figure 4** Box plots comparing the absolute errors between the mean total deviation  
492 (mTD) estimated from cpRNFLT and/or cpVD and the actual mTD. The mean absolute  
493 error with both cpRNFLT and cpVD ( $4.56 \pm 3.76$  dB) was significantly less than that  
494 with cpRNFLT solely ( $5.39 \pm 4.00$  dB,  $p = 0.027$ ) and not significantly less than that  
495 with cpVD solely ( $5.17 \pm 4.08$  dB) ( $p = 0.142$ ). The model for estimating mTD from all  
496 cases with both cpRNFLT and cpVD is as follows:  $mTD = -84.4 + 1.12 \times cpVD$   
497 (standard error (SE) = 0.188,  $p < 0.001$ ) +  $0.233 \times cpRNFLT$  (SE = 0.0435,  $p < 0.001$ ).  
498 The model for estimating mTD from all cases with cpRNFLT alone is:  $mTD = -36.4 +$   
499  $0.367 \times cpRNFLT$  (SE = 0.0426,  $p < 0.001$ ). The model for estimating mTD from all  
500 cases with cpVD alone is:  $mTD = -94.3 + 1.65 \times cpVD$  (SE = 0.180,  $p < 0.001$ ).

501 cpRNFLT: circumpapillary retinal nerve fiber layer thickness; cpVD: circumpapillary  
502 vessel density; SE: standard error  
503





**A****normal vs glaucoma****B****normal vs early****C****early vs moderate****D****moderate vs severe**

**A****B**